*J. Cell Sci.* **20**, 1–20 (1976)
*Printed in Great Britain*



# CRITICAL DENSITY FOR RELAYING IN *DICTYOSTELIUM DISCOIDEUM* AND ITS RELATION TO PHOSPHODIESTERASE SECRETION INTO THE EXTRACELLULAR MEDIUM

A. R. GINGLE
*Departments of Physics and of Biophysics and Theoretical Biology, University of Chicago, Chicago, Illinois* 60637, *U.S.A.*

## SUMMARY

The critical cell density for relaying in *D. discoideum*, $N^*$, has been measured as a function of cell density, $N$, and time after harvesting, $t$. It has logarithmic dependence on $N$ for $2{\cdot}5 \times 10^4/\text{cm}^3 < N < 7{\cdot}5 \times 10^5/\text{cm}^3$ and saturates for $N > 1{\cdot}0 \times 10^6/\text{cm}^3$. $N^*$ is an increasing function of time after harvesting. The phosphodiesterase (PDE) secretion rate on which $N^*$ depends is a constant. Expressions were derived which relate $N^*$ to PDE secretion and diffusion. They have been fitted to the data from time delay experiments yielding values of the PDE diffusion constant in 2% buffered agar, $D_p = (2{\cdot}25 \pm 0{\cdot}15) \times 10^{-9}$ cm$^2$/s, and the ratio of relaying threshold concentration to signal pulse size, $C^*/\eta = (1{\cdot}4 \pm 0{\cdot}05) \times 10^5$ cm$^{-3}$. $N^*$ has also been measured in the presence of various amounts of added beef heart PDE. The cAMP relaxation rates, $1/\tau_0$, due to beef heart PDE were calculated from the $N^*$ measurements and found to be proportional to amounts of added PDE for $(1/\tau_0)\text{max} < (10\ \text{s}^{-1})$. Finally, two kinds of inhibition have been observed in the PDE secretion. The PDE activity per cell is constant for $N < 8{\cdot}0 \times 10^4/\text{cm}^3$, and decreases for larger $N$. It depends only on $N$ for $1/\tau_0 < 10\ \text{s}^{-1}$ and is strongly inhibited by extracellular PDE activity above this relaxation rate.

## INTRODUCTION

*D. discoideum* amoebae aggregate by chemotaxis (Bonner, 1947; Cohen & Robertson, 1971*b*). The chemotactic agent is probably cAMP (Konijn, Barkley, Chang & Bonner, 1968), and in sufficiently dense fields of amoebae the cAMP signal is relayed as a pulse from cell to cell (Shaffer, 1962; Cohen & Robertson, 1971*a*). The signal relaying leads to the characteristic streaming pattern of aggregation in this species (Shaffer, 1962; Gerisch, 1968). In order for relaying to occur there must be spontaneous signalling by some cells (Konijn & Raper, 1961). When spontaneous (autonomous) signals are released they must be large enough to exceed a threshold concentration. If, as seems likely, all signals have the same amplitude, then there will be a critical density of sensitive amoebae below which the aggregative signal cannot be propagated (Cohen & Robertson, 1971*a*). At densities above the critical density the relaying mechanism leads to propagated waves of cAMP concentration, spreading away from autonomous cells. This gives rise to the familiar inward waves of periodic cell movement, noticed by many authors in time-lapse films (see Bonner, 1967).

Below the critical density aggregation is primarily by chemotaxis without signal relaying, because the threshold signal concentration for stimulating chemotaxis is lower than that for stimulating signal relaying (Konijn *et al.* 1968; Robertson & Drage, 1975). Thus, many small aggregates arise, each autonomous cell attracting its neighbours within its chemotactic range. Above the critical density signal relaying occurs enabling each autonomous centre to attract amoebae over large distances (Hashimoto, Cohen & Robertson, 1975). Also, there can be competition between, and entrainment of, neighbouring autonomous centres. This leads to an increase in aggregate territory size with a corresponding reduction in aggregate and fruiting body densities. Several authors have noticed this reduction in fruiting body density (Sussman & Ennis, 1959; Sussman & Sussman, 1961; Bonner, 1967).

All the properties that the amoebae display during aggregation are developed by differentiation, during interphase, which begins when the food supply is exhausted (Shaffer, 1962; Bonner, 1963; Cohen & Robertson, 1972). In the laboratory interphase can be started by centrifuging the amoebae free of their bacterial food supply and plating them, at appropriate densities, on buffered agar. Under these conditions the amoebae first become chemotactically sensitive to cAMP, then capable of relaying a cAMP signal and finally of initiating autonomous signals (Robertson & Cohen, 1974). In order to perform proper biochemical and genetic analysis of signal propagation it is necessary to measure the rate at which each of these aggregative competences is acquired. In the following paper I report measurements of $X_2(t)$, the proportion of amoebae capable of relaying as a function of time after starvation. Basic to these measurements is a knowledge of critical density which is a function of total cell density and time after starvation. This is because the signal is destroyed by an extracellular phosphodiesterase secreted by the amoebae (Chang, 1968), and PDE activity is an increasing function of cell density and time after starvation. The PDE activity shortens the signal range, and therefore increases the critical density, which must be taken into account in the $X_2(t)$ measurements.

In this paper I therefore report the results of experiments to measure critical density and to determine its dependence on the effects of PDE activity. PDE activity is expressed as cAMP conversion rate per cell and as a cAMP relaxation rate. The relaxation rate was used because, for linear enzyme kinetics, it is the ratio of maximal conversion rate to the Michaelis–Menton constant ($V_{max}/K_m$) and thus affords a convenient measure of activity. In physical terms it is the rate of cAMP conversion per molecule of cAMP. It was necessary to determine the rate at which PDE activity increased from the beginning of interphase for each cell density and to estimate the distribution of PDE activity in the agar on which the amoebae were placed. Thus, while the idea behind the experiments was simple, their execution was quite complicated. I therefore give an outline of the sequence of experiments performed, and of the purpose of each experiment, before describing the results.

METHODS

## *Culturing*

Growth cultures of *D. discoideum* (NC-4) (a wild type haploid strain obtained from Prof. K. B. Raper), and D1 (a non-aggregating mutant derived by A. J. Durston by u.v. irradiation of strain Ax-2) (Ashworth & Watts, 1970), were prepared by inoculating suspensions of *Aerobacter aerogenes* with either *D. discoideum* spores or D1 cells (as D1 never forms spores) and plating them on to nutrient agar growth plates. The cultures were incubated at 22 °C; *D. discoideum* cultures for 30 h and the slower growing D1 cultures for 80 h. Amoebae were washed from plates in cold phosphate buffer and separated from the food bacteria by differential centrifugation. The amoebae were resuspended in buffer and diluted to the desired concentration using a haemocytometer. Appropriate volumes of the *D. discoideum* and D1 suspensions were plated on to $0{\cdot}5 \times 1{\cdot}0$ cm blocks of 2 % agar made up in phosphate buffer (pH 6·5).

## *Plating*

The buffered agar blocks were placed in 10-cm diameter plastic Petri dishes, 6 to a dish. Each dish contained a water-soaked filter paper to maintain proper humidity for culmination (Raper, 1940). In each experiment volumes of *D. discoideum* and D1 cell suspensions were deposited separately on to each agar block. The volumes of the *D. discoideum* suspensions were chosen so that the series of blocks would contain a range of *D. discoideum* densities, $N_R$, in steps of $1{\cdot}0 \times 10^3/\text{cm}^2$. Increased density due to cell divisions after harvesting was taken into account by reducing the suspension concentrations to 83 % of their nominal values. The volumes of the D1 suspensions were chosen so that the total cell density on each block, $N = N_R + N_{D1}$, would be constant at the value set in the experiment. All cell densities were measured to an accuracy of $\pm 5$ %. When both the *D. discoideum* and D1 amoebae were plated, the Petri dishes were sealed with masking tape and kept at 22 °C. The mixed populations were then allowed to pass through their entire life cycle to culmination before measurements were taken, usually 80 h to 100 h later.

## *Filming*

Filming by time-lapse cinemicrography was carried out as previously described (Robertson, Drage & Cohen, 1972) and as in the accompanying paper (Gingle & Robertson, 1975).

## *Measurement*

Measurements were made by counting the total number of aggregates or fruiting bodies on each agar block. The aggregates or fruiting bodies were observed with a Nikon microscope set at a magnification of 20. The aggregate or fruiting body densities were then plotted as functions of $N_R$, the density of *D. discoideum* amoebae.

## *Theory of measurements*

In mixed populations there are 2 regions of $N_R$ in which aggregation morphologies are quite distinct. The 2 regions are separated by the critical density for long range relaying, $N^*$ (Hashimoto *et al.* 1975). For $N_R < N^*$ no long-range signal relaying occurs. Therefore, aggregation consists of autonomous cells attracting amoebae into small clusters via chemotaxis with only local signal relaying. Here the term cluster means a set of amoebae, all within a relay range, $R$, of each other. Amoebae near the clusters are attracted into them by chemotaxis since the chemotactic range is greater than the relay range. However, the amoeba density in the field decreases until even chemotaxis becomes ineffective. As a result, autonomous centres have small aggregation territories and develop independently into small aggregates of which a portion become fruiting bodies.

The results of percolation theory can be directly applied to this system if we consider a field with uniform amoeba density and infinite amoeba number. In this case percolation theory predicts that as $N_R$ increases towards $N^*$ the mean cluster size tends to infinity (Shante &

Kirkpatrick, 1971). Thus for $N_R > N^*$ there exist percolation channels, within which amoebae are close enough together for signal relaying, that extend throughout the field. As autonomous cells emerge, they attract amoebae from the 'infinite' cluster by relaying along the percolation channels. Amoebae outside the cluster are attracted into it by chemotaxis towards the percolation channels. Eventually the field breaks up into large aggregation territories with refractory boundaries between them (Cohen & Robertson, 1971*a*, *b* and Hashimoto *et al.* 1975).

Therefore, as $N_R$ passes through $N^*$, the aggregation morphology changes sharply from one of many small aggregation territories with small aggregates and fruiting bodies to one of large aggregation territories with relatively few aggregates and fruiting bodies. There is a sharp increase in mean aggregation territory size at $N^*$ with a correspondingly sharp decrease in aggregate and fruiting body densities. It is this discontinuity which appears in the aggregate and fruiting body density curves, and yields the values of $N^*$. This phenomenon has been observed by several authors (Sussman & Noel, 1952; Shaffer, 1962).

### *Typical experiment*

There were 5 different experimental procedures employed to yield the data. They are summarized in Table 1 and described below:

(1) The single harvest experiment was simply to measure the critical density for a particular total cell density. In these experiments the *D. discoideum* and D1 populations were harvested and plated together. That is, development of the *D. discoideum* and the D1 amoebae was synchronized.

Table 1. *Summary of experimental procedures*

| Experiment | Harvesting time | | Plating time | | PDE addition time |
|---|---|---|---|---|---|
| | Dd | D1 | Dd | D1 | |
| 1 | 0 | 0 | 0 | 0 | — |
| 2 | 0 | $0 < t < 600'$ | 0 | $0 < t < 600'$ | — |
| 3 | 0 | 0 | 0 | $0 < t < 600'$ | — |
| 4 | 0 | 0 | 0 | 0 | 0 |
| 5 | 0 | 0 | 0 | 0 | $0 < t < 600'$ |

Thus, NC-4 was always plated at $t = 0$, while harvesting and plating times for $D_1$ were independently varied, as was the time of phosphodiesterase application.

(2) The multiple harvest time delay experiments were done to measure $N^*$ at various times after harvesting. The data from these experiments were used to calculate the parameters $D_p$ and $C^*/\eta$, where $D_p$ is the diffusion constant of PDE in 2 % buffered agar and $C^*/\eta$ is the ratio of threshold cAMP concentration for relaying to the number of molecules in each signal pulse. In these experiments the D1 populations were harvested and plated a fixed delay time after the *D. discoideum* population. This procedure was repeated for delay times ranging from 0′ to 600′, total cell density being held constant.

(3) The single harvest time delay experiments were done to test for any explicit time-dependence of the slime mould PDE secretion rate. In these experiments the D1 population was harvested at the same time as the *D. discoideum* population, but was recentrifuged and plated a delay time after the *D. discoideum* amoebae, which had been plated shortly after harvesting. This procedure was also repeated for delay times ranging from 0′ to 600′ with total cell density held constant.

(4) The PDE addition experiments were done to measure the effect of PDE level on the PDE secretion rate. These experiments were similar to the single harvest experiment with one exception. Fixed amounts of beef heart PDE were applied to the surface of each agar block shortly before plating the amoeba populations. The experiment was repeated with different amounts of added PDE ranging from 1 to 20 $\mu g/cm^2$.

(5) PDE addition experiments were also performed with the application of beef heart PDE at times after harvesting ranging up to 600′. Data from these experiments were used to determine the beef heart PDE diffusion constant in 2 % buffered agar.

## RESULTS

### *General features*

Typical aggregate and fruiting-body density curves, obtained by single harvest experiments, are shown in Fig. 1. The first 2 are plots of aggregate density, $N_A$ vs. $N_R$ for $N = 5 \times 10^5/cm^2$ and $10^6/cm^2$ and the latter 2 are plots of fruiting body density, $N_{fb}$ vs. $N_R$ for $N = 10^5/cm^2$ and $10^6/cm^2$. $N_{fb}$ is considerably smaller than $N_A$ for the *D. discoideum* D1 mixtures except for $N_R/N$ close to unity. However, both types of curve exhibit similar structure. The curves exhibit the sharp decrease at $N_R = N^*$. They are increasing for $N_R < N^*$ and relatively constant for $N_R > N^*$ (Sussman & Sussman, 1961; Bonner & Dodd, 1962).

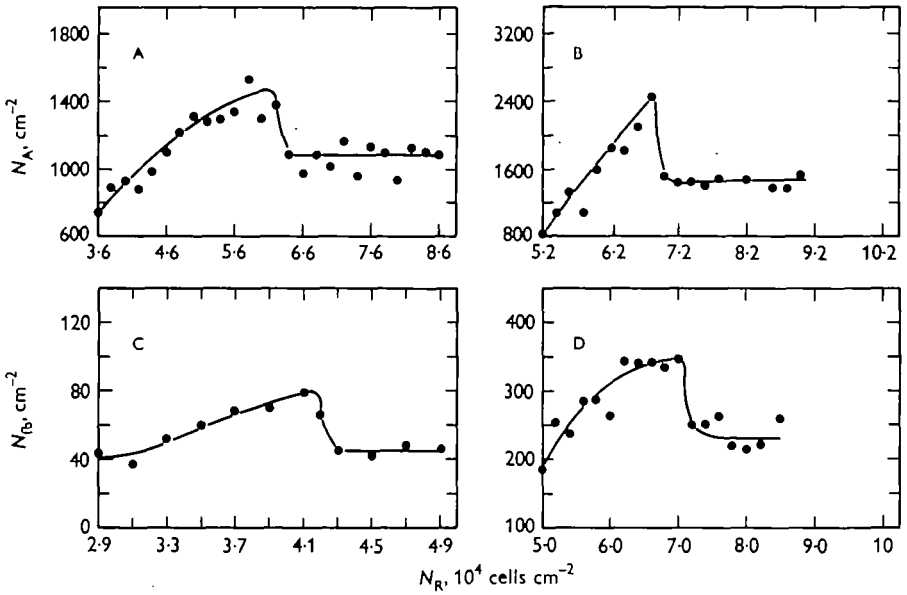


Fig. 1. Typical aggregate and fruiting body density curves. The graphs represent: A, $N_A$ vs. $N_R$ for $N = 5{\cdot}0 \times 10^5/cm^2$; B, $N_A$ vs. $N_R$ for $N = 1{\cdot}0 \times 10^6/cm^2$; C, $N_{fb}$ vs. $N_R$ for $N = 1{\cdot}0 \times 10^5/cm^2$; and D, $N_{fb}$ vs. $N_R$ for $N = 1{\cdot}0 \times 10^6/cm^2$.

### *Dynamics*

Various mixtures of *D. discoideum* and D1 cells were filmed, many with cAMP pulsed from microelectrodes placed in the field. This was done to observe the onset of long-range relaying. The following general features were observed. Fields with $N_R > N^*$ had a characteristic relaying onset time $t^*$, observed in 2 ways. The first was pulsatile movements of the D1 amoebae beginning at $t^*$. The non-relaying and non-refractory D1 amoebae jitter forward and backward as the signal relayed by the wild-type amoebae

passes. This jitter of the D1 amoebae masks the cell movement waves normally observed in wild-type populations (Bonner, 1967). The second was a rapid clearing of the field by a microelectrode beginning at $t^*$. In these cases the attraction to the microelectrode extended far beyond its chemotactic range. The third was the breaking up of the field into high and low density regions. This was caused by an attraction between amoebae probably due to cAMP leakage from the D1 amoebae and was enhanced at $t^*$ by relaying. It occurred irrespective of artificial cAMP pulsing.

*$N^*$ vs. $N$*

Culmination density experiments were done over a wide range of cell densities ($2{\cdot}5 \times 10^4/\text{cm}^2 < N < 2 \times 10^6/\text{cm}^2$). For each total cell density $N$, $N^*$ was determined via the discontinuity in $N_A$ or $N_{fb}$. When only wild-type amoebae are plated, $N = N_R$,

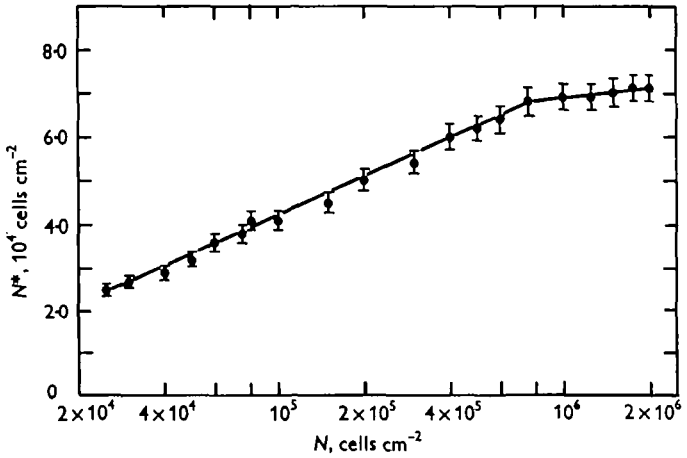


Fig. 2. Critical density vs. total cell density at 620 min after harvesting.

the discontinuity appears at $N = N_R = 2{\cdot}5 \times 10^4/\text{cm}^2$. This is the limiting value of critical density at which $N^* = N$. It is also the lowest cell density in which long-range signal relaying will occur (Gingle & Robertson, 1975). The critical density data are plotted as a function of $N$ in Fig. 2. The data exhibit a logarithmic dependence on $N$ for $N < 7{\cdot}5 \times 10^5/\text{cm}^2$ and saturate for greater $N$. For $N < 7{\cdot}5 \times 10^5/\text{cm}^2$, the data have been fitted to the following equation

$$N^* = N_1^* \ln N + N_2^*, \tag{1}$$

where the best fit was obtained for $N_1^* = 1{\cdot}19 \times 10^4\,\text{cm}^{-2}$ and $N_2^* = -9{\cdot}56 \times 10^4\,\text{cm}^{-2}$, with $\chi^2 = 4{\cdot}8$ and the corresponding confidence level $P = 0{\cdot}98$. The percolation equation, $\pi R^2(N)N^* = 4{\cdot}5$, relating cAMP signal range to critical density (Cohen & Robertson, 1975), was used to compute signal range, $R$, from $N^*$. A plot of $R(N)$ is shown in Fig. 3. As the results of the Time delay experiments will show, the $N^*(N)$ and $R(N)$ data in Figs. 2 and 3 correspond to a time of approximately 620′ after harvesting.

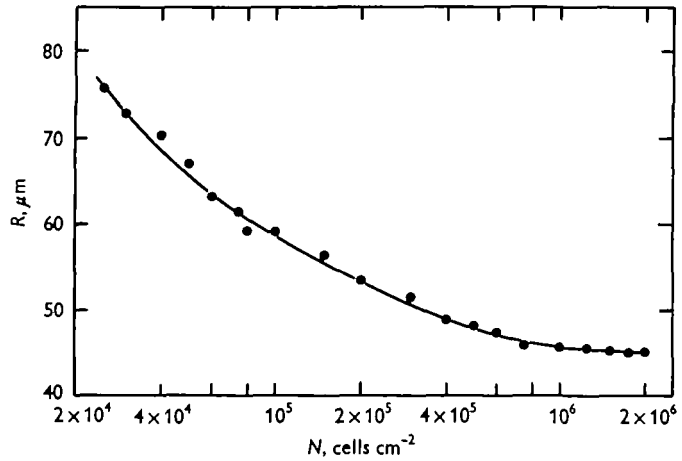


Fig. 3. Signal range vs. total cell density at 620 min after harvesting.

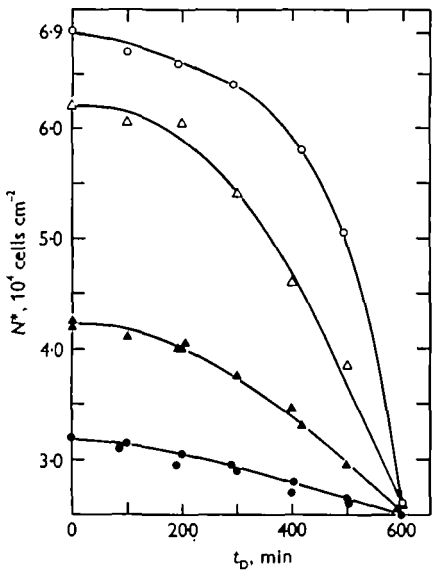


Fig. 4

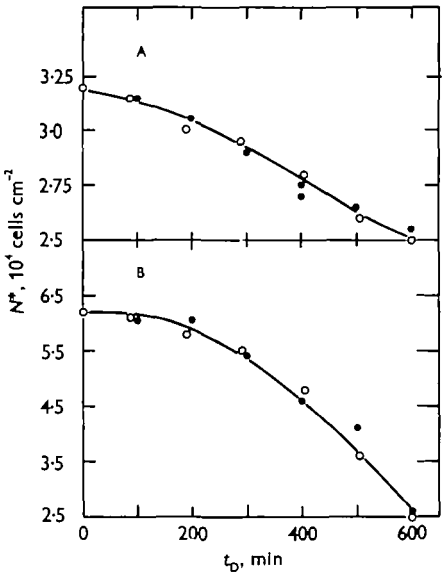


Fig. 5

Fig. 4. Critical density vs. time delay for multiple harvest time delay experiments. —●—●—, $N = 5 \times 10^4/cm^2$; —▲—▲—, $N = 1{\cdot}0 \times 10^5/cm^2$; —△—△—, $N = 5 \times 10^5/cm^2$; and —○—○—, $N = 1{\cdot}0 \times 10^6/cm^2$.

Fig. 5. Comparison of single harvest and multiple harvest time delay data. The graphs represent: A, $N = 5{\cdot}0 \times 10^4/cm^2$, and B, $N = 5{\cdot}0 \times 10^5/cm^2$. —●—●—, multiple harvest and —○—○—, single harvest.

*Time delay experiments*

The results of the multiple harvest experiments will be described first. These are the experiments (2 and 3) in which populations of D1 were harvested at successive time delays $t_1$, (0, 100′, 200′, 300′, 400′, 500′, and 600′) after *D. discoideum* harvesting. The critical densities of these mixtures were determined in the usual manner and plotted

with respect to $t_D$. These time delay experiments were performed for $N = 5 \times 10^4/cm^2$, $10^5/cm^2$, $5 \times 10^5/cm^2$, and $10^6/cm^2$. The data are shown in Fig. 4. They indicate that $N^*$ is a decreasing function of $t_D$ and that at $t_D = 600'$ the $N^*$'s in all 4 data sets are approximately $2{\cdot}5 \times 10^4/cm^2$, the limiting and smallest value of $N^*$ (Gingle & Robertson, 1975).

In the single harvest experiments, the D1 populations were harvested along with the *D. discoideum*. However, the D1 populations were plated at successively longer $t_D$'s after the *D. discoideum* population. These experiments were performed at 2 densities: $N = 5 \times 10^4/cm^2$ and $5 \times 10^5/cm^2$. The data are plotted along with the corresponding multiple harvest data in Fig. 5 A, B. The multiple harvest and single harvest data are essentially identical.

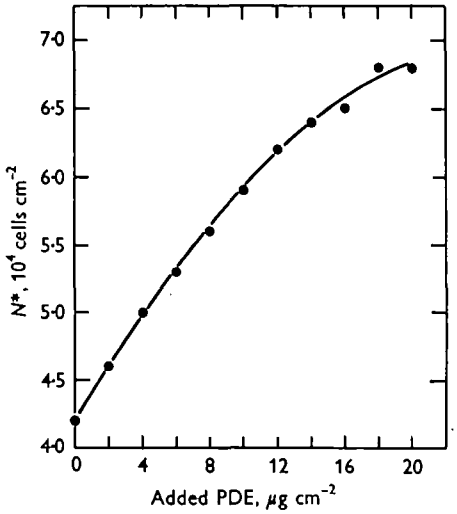


Fig. 6. Critical density vs. added beef heart PDE ($\mu g/cm^2$) with $N = 1{\cdot}0 \times 10^5/cm^2$.

*Addition of beef heart PDE*

Critical densities were measured for fields of $N = 10^5/cm^2$ in the presence of beef heart PDE. The beef heart PDE was added at harvesting in amounts ranging from 1 to 20 $\mu g/cm^2$. Critical densities are plotted with respect to amount of added PDE in Fig. 6. $N^*$ is an increasing function of added PDE, ranging from $4{\cdot}1 \times 10^4/cm^2$ with no added PDE, to $7{\cdot}0 \times 10^4/cm^2$ with 20 $\mu g/cm^2$. The latter value of $N^*$ is normally characteristic of $N = 1{\cdot}5 \times 10^6/cm^2$.

In addition, critical densities were measured for fields with beef heart PDE added at various times after harvesting. Amounts, 2 $\mu g/cm^2$ and 4 $\mu g/cm^2$, of beef heart PDE were added at times up to 600'. For 2 $\mu g/cm^2$, $N^*$ ranged from $4{\cdot}6 \times 10^4/cm^2$ with application at harvesting, to $5{\cdot}8 \times 10^4/cm^2$ with application 600' after harvesting.

## DISCUSSION

*General features*

The aggregate and fruiting body density curves of Fig. 1 exhibit 2 distinct regions, $N_R < N^*$ and $N_R > N^*$. In the first region, $N_R$ is not sufficiently large for long-range

signal relaying so aggregation occurs over a short range primarily via chemotaxis. Each autonomous centre attracts amoebae from a small surrounding area with little interaction between centres. Because of this lack of interaction between centres and because D1 amoebae are incapable of autonomy, $N_A$ and $N_{fb}$ are increasing functions of $N_R$. For $N_R > N^*$, long-range signalling occurs via relaying and therefore autonomous centres can attract amoebae over large distances via relaying along percolation channels. Aggregation territories are considerably larger than for $N_R < N^*$. Correspondingly, $N_A$ and $N_{fb}$ are sharply reduced from their values at $N_R < N^*$ and are relatively constant over the regions of $N_R$ studied.

*Internal consistency*

The time-lapse films of *D. discoideum*/D1 mixtures yielded characteristic onset times, $t^*$, for long-range signal propagation. These data offer a means of determining how closely the PDE activity of the D1 cells mimics that of wild-type amoebae. Each $t^*$ is characteristic of 2 parameters: $N$, total cell density, and $N_R$, partial density of NC-4,

Table 2. *Internal consistency check on the equality of the wild-type D. discoideum and* D1 *PDE secretion rates*

| $N$, cm$^{-2}$ | $X_R$ | $t^*$, min | $X_1^*$ | $N^*(t^*)$, cm$^{-2}$ | $\frac{NX_2^*X_R}{N^*}$ |
|---|---|---|---|---|---|
| $5{\cdot}0 \times 10^4$ | 0·7 | 572 | 0·96 | $3{\cdot}25 \times 10^4$ | $1{\cdot}03 \pm 0{\cdot}07$ |
| $2{\cdot}5 \times 10^5$ | 0·75 | 498 | 0·3 | $5{\cdot}36 \times 10^4$ | $1{\cdot}05 \pm 0{\cdot}19$ |
| $5{\cdot}0 \times 10^5$ | 0·5 | 467 | 0·23 | $5.8 \times 10^4$ | $0{\cdot}99 \pm 0{\cdot}14$ |
| $5{\cdot}0 \times 10^5$ | 0·13 | 550 | 0·92 | $6{\cdot}0 \times 10^4$ | $1{\cdot}00 \pm 0{\cdot}09$ |
| $1{\cdot}0 \times 10^6$ | 0·75 | 323 | 0·08 | $5{\cdot}7 \times 10^4$ | $1{\cdot}05 \pm 0{\cdot}19$ |
| $1{\cdot}0 \times 10^6$ | 0·5 | 419 | 0·13 | $6{\cdot}15 \times 10^4$ | $1{\cdot}05 \pm 0{\cdot}14$ |
| $1{\cdot}0 \times 10^6$ | 0·5 | 420 | 0·12 | $6{\cdot}15 \times 10^4$ | $0{\cdot}98 \pm 0{\cdot}13$ |
| $1{\cdot}0 \times 10^6$ | 0·07 | 535 | 0·84 | $6{\cdot}6 \times 10^4$ | $0{\cdot}93 \pm 0{\cdot}13$ |
| $2{\cdot}0 \times 10^6$ | 0·5 | 317 | 0·07 | $7{\cdot}1 \times 10^4$ | $0{\cdot}99 \pm 0{\cdot}2$ |

relaying cells. For each field the density of relaying-competent cells at $t^*$ is $NX_2(t^*)X_R$, where $X_2(t^*)$ is the fraction of those NC-4 cells which are relaying competent by $t^*$ and $X_R = N_R/N$. At the onset time the density of relaying-competent cells equals $N^*$ or

$$NX_2(t^*)X_R = N^*, \tag{2}$$

which can be rewritten as

$$\frac{NX_2(t^*)X_R}{N^*} = 1. \tag{3}$$

These equations assume that NC-4 and D1 have the same PDE secretion rate as well as any other factors which influence $N^*$. The $X_2(t)$ values are taken from the NC-4 $X_2(t)$ curve (Gingle & Robertson, 1975) while the $N^*$ and $t^*$ values are from experiments with NC-4/D1 mixtures.

This offers an internal consistency check between the 2 sets of measurements. The experimental values of $NX_2(t^*)X_R/N^*$ are listed in Table 2. They are essentially constant and equal to 1 with a $\chi^2 = 0{\cdot}99$ and confidence level $P = 1{\cdot}0$. Thus a most

important point has been verified. That is, the D1 cells do indeed mimic the wild-type PDE secretion. Therefore any critical density data taken from NC-4/D1 mixtures will apply equally to populations of NC-4 alone.

*PDE secretion rate vs. cell density and time*

The first order theory of relay range, discussed in the Appendix to this paper, was used to calculate PDE secretion rates from the data of Fig. 2. Equations (11) and (12*a*) of the Appendix were used for these calculations. However, before describing this, some properties of the $N^*$ measurements and PDE secretion rates must be established. The first property to establish is the time to which the $N^*$ measurements of Fig. 2 correspond. This can be established from the time delay data of Fig. 4. Recall that at $t_D \simeq 600'$ we have $N^* \simeq 2{\cdot}5 \times 10^4/\text{cm}^2$, for $5{\cdot}0 \times 10^4/\text{cm}^2 < N < 10^6/\text{cm}^2$. The D1 cells, harvested and plated at $t_D$, secrete PDE into the field over a period from $t_D$ to $t_R$, the time in the life cycle when the uniform field breaks up via relaying if $N_R > N^*$. When $t_D = t_R$ the D1 population does not contribute to either the PDE activity or $N^*$. The mixed populations are in effect only wild-type populations of total density $N_R$. Thus the discontinuity in $N_A$ and $N_{fb}$ occurs at the limiting value of critical density, $2{\cdot}5 \times 10^4/\text{cm}^2$. As shown in Fig. 4 this occurs at $t_R \simeq 600'$ irrespective of $N$.

The second property to establish is the explicit time-dependence of the PDE secretion rate. A comparison of the single and multiple harvest time delay data (Fig. 5) offers a means of determining the time-dependence. In the single harvest experiments all of the D1 populations are harvested at $t = 0$ and initiate their development then. However, in the multiple harvest experiments each D1 population starts its development at a different $t_D$. There are therefore temporal phase shifts of $t_D$ between corresponding D1 populations of the 2 experiments. The development of D1 populations in the multiple harvest experiments have time lags of $t_D$ behind the development of the corresponding D1 populations in the single harvest experiments. Because of the temporal phase shifts, the multiple harvest and single harvest experiments will yield identical $N^*$'s only if the PDE secretion rate is invariant under temporal shifts, i.e. is constant with respect to time. The multiple harvest and single harvest data are essentially identical and therefore the PDE secretion rate, $G$, has no explicit time dependence.

PDE secretion rate, $G$, is calculated in terms of $G' = n_s k_3 G/K_m$, where $K_m$ is the Michaelis–Menten constant of PDE in the system, $k_3$ is the dissociation rate of the enzyme–substrate complex, and $n_s$ is the number of active sites per PDE molecule. The secretion rate, as calculated by the theory, is shown in Fig. 7. The plot exhibits three clearly separated regimes. In the first, $N < 8{\cdot}0 \times 10^4/\text{cm}^2$, the secretion rate is constant. In the second, $8{\cdot}0 \times 10^4/\text{cm}^2 < N < 7{\cdot}5 \times 10^5/\text{cm}^2$, the secretion rate is proportional to $N^{-\frac{1}{2}}$. That is the secretion rate is proportional to the mean amoeba separation. In the third regime, $N > 7{\cdot}5 \times 10^5/\text{cm}^2$, $G'$ decreases more rapidly with increasing $N$. The maximal activity of PDE secreted per cell is proportional to $G'$. It has been calculated and expressed in standard biochemical units (pmol/min/cell). This was done using a value of 10 $\mu$M for the $K_m$ of slime mould PDE (Malkinson & Ashworth, 1973). These maximal activities per cell are plotted as a function of $N$ in Fig. 7 along with $G'$. The values are maximal activities of PDE secreted per cell over a 620′ period from harvesting.

The calculated values of PDE secretion rates and levels can be correlated with the results of biochemical assays when they become available. This convenient technique offers an alternative to conventional biochemical methods for *in vivo* assaying.

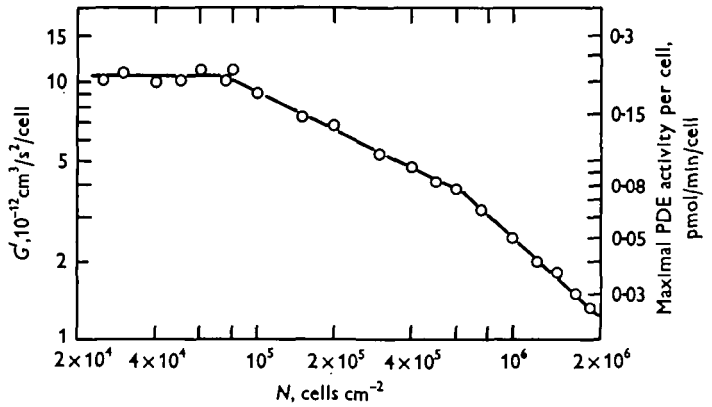


Fig. 7. PDE secretion rate and maximal PDE activity per cell at 620 min vs. total cell density.

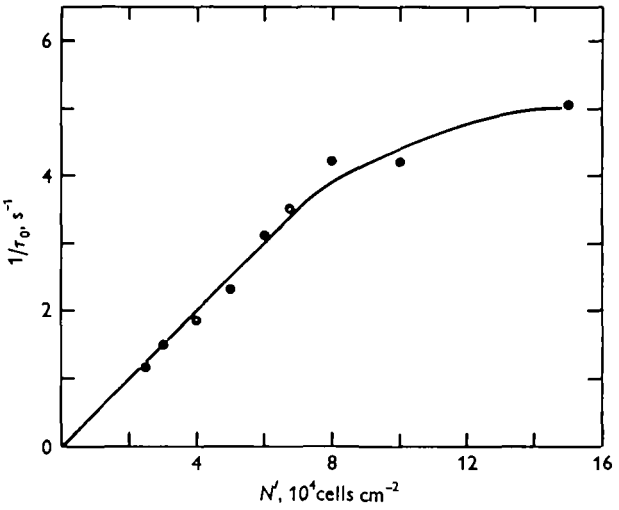


Fig. 8. cAMP surface relaxation rate vs. total cell density.

The cAMP relaxation rate at the surface is also plotted in Fig. 8. For $N < 8{\cdot}0 \times 10^4$/cm$^2$, $G'$ is constant and $1/\tau_0 \propto N$. This offers further evidence that the wild-type and D1 PDE secretion rates are equal. For, if the secretion rates are assumed to be unequal, $1/\tau_0$ has the form

$$\frac{1}{\tau_0} = \gamma_{Dd} N^* + \gamma_{D1}(N - N^*) \tag{4}$$

for the critical density measurements. Here $\gamma_{Dd}$ and $\gamma_{D1}$ are the relaxation rates per

unit density for NC-4 and D1 respectively. Since $N^*$ is given by Equation (1) of the previous section, we have for $1/\tau_0$

$$\frac{1}{\tau_0} = \gamma_{D1}N + (\gamma_{Dd} - \gamma_{D1})N_2^* + N_1^*(\gamma_{Dd} - \gamma_{D1}) \ln N. \tag{5}$$

This expression for $1/\tau_0$ not only contains a linear term but also contains a constant and a logarithmic term in $N$. However, if $\gamma_{Dd} = \gamma_{D1}$ this equation reduces to

$$\frac{1}{\tau_0} = \gamma_{Dd}N \tag{6}$$

which is observed for $N < 8{\cdot}0 \times 10^4/\text{cm}^2$, as the fit to the data in this portion of the curve yields $\chi^2 = 1{\cdot}38$ with $P = 0{\cdot}96$. The sensitivity of the experimental technique was such that relative differences between $\gamma_{Dd}$ and $\gamma_{D1}$ of 5 % could easily be detected.

*$D_p$ and $C^*/\eta$*

The first-order relay range theory, discussed in the Appendix to this paper, was fitted to the $5 \times 10^4/\text{cm}^2$ and $10^5/\text{cm}^2$ multiple harvest time delay data. (Equations (11)

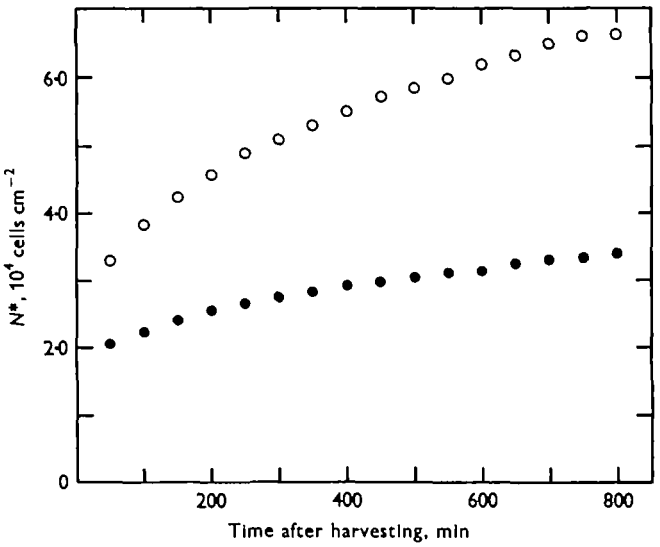


Fig. 9. Expected critical density vs. time after harvesting as calculated from theory. ● ●, $N = 5{\cdot}0 \times 10^4/\text{cm}^2$; and ○ ○, $N = 5{\cdot}0 \times 10^5/\text{cm}^2$.

and (12*b*) of the Appendix were used for these calculations.) The parameters $D_p$, $C^*/\eta$ and $G'$ were varied on the computer over wide ranges of possible values. A $\chi^2$ fit to the data was done for each set of parameters. The minimum $\chi^2 = 12{\cdot}6$ was calculated with

$$D_p = (2{\cdot}25 \pm 0{\cdot}15) \times 10^{-9}\,\text{cm}^2/\text{s} \quad \text{and} \quad C^*/\eta = (1{\cdot}4 \pm 0{\cdot}5) \times 10^5\,\text{cm}^{-3}.$$

The corresponding confidence level was $P = 0{\cdot}96$. The values of $G'$ are in agreement with those shown in Fig. 7. With the values of the parameters known, $N^*(t)$ can now be calculated. Critical density vs. time curves for $N = 5 \times 10^4/\text{cm}^2$ and $5 \times 10^5/\text{cm}^2$ are

shown in Fig. 9. $N^*$ is now completely determined as a function of both $N$ and $t$. The ratio of the first order to zeroth order cAMP concentration is $C_1/C_0 < 0{\cdot}09$. It is small as required for accuracy with the first-order approximation.

*PDE addition experiments*

The $N^*$ data (Fig. 6) from the PDE addition experiments make a direct test of the relaying range theory possible. The cAMP relaxation rate, $1/\tau$, can be calculated from Equations (11) and (12*c*) of the Appendix and has 2 components: one, due to PDE from the continuously secreting amoebae, and the other, the beef heart PDE activity added at time zero. The 2 components can be separated by their different spatial dependence

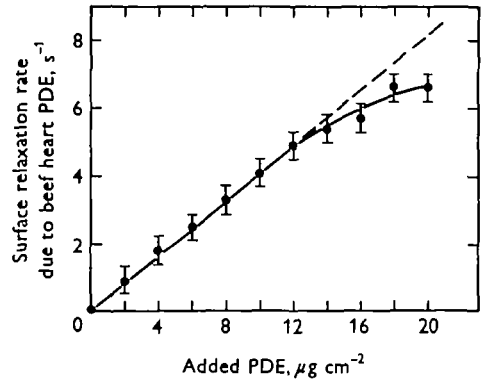


Fig. 10. Surface relaxation rate for cAMP vs. added beef heart PDE ($\mu$g/cm$^2$) with $N = 1{\cdot}0 \times 10^5$/cm$^3$.

and therefore the relaxation rate due to added beef heart PDE can be determined. The relaxation rate at the surface due to beef heart PDE, is plotted with respect to amount of PDE added per unit area of agar surface (Fig. 10). In the calculations for this plot the PDE secretion rate of the amoebae was artificially held constant. Thus any non-linearity is actually due to a reduction in $G'$. The plot is proportional to added PDE for total relaxation rates, $1/\tau_0 < 10\,s^{-1}$. The high PDE levels for early times after applying the beef heart PDE seemed to have little effect. Thus the calculated amount of PDE, measured in terms of cAMP relaxation rate, is proportional to the actual amount added. This result offers further evidence for cAMP as the relayed signal. It also is a direct and crucial test of the theory. The beef heart PDE diffusion constant in 2 % agar has been calculated using the dependence of $N^*$ on PDE application time. The value of the beef heart diffusion constant is $D_P = (7{\cdot}1 \pm 0{\cdot}5) \times 10^{-10}$cm$^2$/s.

*Properties of D1*

The following is a list of D1 properties illustrated by this work. The first 2 were also observed in Durston's time-lapse film.

(1) D1 cannot relay a signal of cAMP. This is evident from the culmination curves of Fig. 1, for if D1 relayed then $N_R$ = constant and the discontinuity would not appear.

(2) D1 does not become autonomous. This can be seen in the increasing, almost linear, dependence of aggregate and fruiting body density on wild-type density (Fig. 1).

(3) D1 probably leaks cAMP at an abnormally high rate sufficient to excite relaying in *D. discoideum*, NC-4.

(4) D1 secretes PDE at normal rates throughout the first 600 min after harvesting.

The technique of mixing mutant and wild-type amoebae has yielded information about both D1 and NC-4 which would have otherwise been difficult to obtain. It should also be useful for a wide range of other mutant–wild-type and mutant–mutant mixtures.

*Inhibition of PDE secretion*

The PDE secretion rate is only constant for $N < 8{\cdot}0 \times 10^4/\text{cm}^2$ (Fig. 7). For larger $N$ it is a decreasing function of cell density. Conceivably, the inhibition in PDE secretion could depend on both cell density and on PDE level which increases with $N$. Any dependence on PDE level will appear as a non-linearity in the PDE addition curve (Fig. 10). I noted in the previous section that the departure from linearity in this curve occurred when $1/\tau_0(620') \simeq 10\,\text{s}^{-1}$. In the $N^*$ vs. $N$ data, $N^*$ departs from its logarithmic dependence on $N$ and saturates at $N \simeq 7 \times 10^5/\text{cm}^2$; this corresponds to the second shift in the slope of the $\ln G'$ vs. $\ln N$ plot (Fig. 7) between $6 \times 10^5/\text{cm}^2$ and $7{\cdot}5 \times 10^5/\text{cm}^2$. The corresponding maximum surface relaxation rate is between $10\,\text{s}^{-1}$ and $11\,\text{s}^{-1}$. Thus the saturation in $N^*$ and the non-linearity in the PDE addition data occur at approximately the same PDE level, $1/\tau_0 \simeq 10\,\text{s}^{-1}$. Therefore, whatever the mechanism, the saturation in $N^*$ is due to a dependence on PDE level. That is, PDE secretion is dependent on PDE level for $1/\tau_0 > 10\,\text{s}^{-1}$ and independent of level for $1/\tau_0 < 10\,\text{s}^{-1}$. The apparent $1/\tau_0$ dependence of $G'$ for $1/\tau_0 > 10\,\text{s}^{-1}$ has an alternative interpretation. That is PDE secretion is not being inhibited by PDE level but that PDE is becoming inactive, perhaps due to dimerization. In either case the almost discrete emergence of level inhibition is an important constraint on any mechanism to explain the behaviour of PDE secretion and inhibition.

Below $1/\tau_0 \simeq 10\,\text{s}^{-1}$ PDE secretion is independent of $1/\tau_0$; however, inhibition occurs and is purely $N$ dependent. This is observed in the second portion of the $\ln G'$ vs. $\ln N$ curve (Fig. 7). This form of inhibition is purely dependent on inter-amoeba separation, $G'$ being proportional to the mean separation.

This work was supported by NIH Grant no. HD-04722, NSF Grant no. GB-30784. It was submitted in satisfaction of the requirements for the Ph.D. degree in Physics, University of Chicago.

I am grateful for suggestions and criticism from Morrell H. Cohen and Anthony Robertson.

SYMBOLS USED IN TEXT

$C$ Concentration of cAMP.
$C^*$ Threshold cAMP concentration for relaying.
$C_0$ Zeroth order cAMP concentration term.
$C_1$ First order cAMP concentration term.

$D$ cAMP diffusion constant in 2 % buffered agar.
$D_{\mathrm{p}}$ Slime mould PDE diffusion constant in 2 % buffered agar.
$D'_{\mathrm{p}}$ Beef heart diffusion constant in 2 % buffered agar.
$F(t)$ Factor in the expression for cAMP concentration which takes the PDE distribution into account.
$G$ PDE secretion rate.
$G'$ k$G$.
$\gamma_{\mathrm{Dd}}$ Proportionality constant between cAMP relaxation rate and cell density for Dd.
$\gamma_{\mathrm{D1}}$ Proportionality constant between cAMP relaxation rate and cell density for D1.
$k_3$ Dissociation rate for the cAMP–PDE complex.
$K_m$ Michaelis–Menten constant for PDE.
$k$ $k_3 n_s/K_m$ for slime mould PDE.
$k'$ $k_3 n_s/K_m$ for beef heart PDE.
$N$ Total amoebae density.
$N^*$ Critical amoebae density for relaying.
$N_{\mathrm{R}}$ Density of amoebae capable of attaining relaying competence.
$N_{\mathrm{D1}}$ Density of D1 amoebae.
$N_{\mathrm{A}}$ Density of aggregates.
$N_{fb}$ Density of fruiting bodies.
$\eta$ Number of molecules per relayed signal pulse.
$n_s$ Number of active sites per PDE molecule.
$R$ Signal range for relaying.
$t_m$ Time of maximum cAMP concentration after an amoeba signals.
$\tau_0$ Mean cAMP lifetime.
$1/\tau_0$ cAMP relaxation rate.
$t_D$ Delay time between harvesting of D1 and Dd amoebae population.
$t^*$ Onset time for long-range signal relaying.
$t_{\mathrm{R}}$ Time after harvesting at which the field breaks up due to cAMP secretion and relaying.
$X_{\mathrm{R}}$ Fraction of amoebae capable to become relaying competent.
$X_2(t)$ Fraction of relaying competent amoebae.

## APPENDIX: FIRST ORDER THEORY OF RELAY RANGE

*General*

Expressions have been formulated for the signal range, $R$, which take into account the spatial distribution of PDE in the agar. The expressions are based on a range theory due to Cohen & Robertson (1974). Their theory was based on the following: (1) a constant relaying threshold cAMP concentration, $C^*$, and cAMP pulse size, $\eta$; (2) hemispherical diffusion of a short cAMP pulse into the agar from the signalling amoebae on the surface; and (3) small cAMP secretion area on the amoeba surface (Robertson & Cohen, 1974). Linear enzyme kinetics were assumed in the derivation of the expressions. Also the cell-

bound PDE was neglected as it has little affect on aggregation for $N < 1{\cdot}0 \times 10^6$cells/cm$^2$. Considering the extracellular PDE activity per cell of 0·05 pmol/min/cell ($N = 1 \times 10^6$ cells/cm$^2$) and the cell-bound PDE activity of 100 nmol/20 min/$10^6$ cells (Henderson, 1975) yields a value for the ratio of cell-bound to extracellular PDE activity at the agar surface. The ratio is 8% for 600′ after harvesting; the extracellular surface activity corresponded to the PDE in a 10-$\mu$m layer below the agar surface. In this work I take into account, in addition, the actual PDE concentration profiles in the agar. The final expressions relating signal range, $R$, and PDE secretion rate, $G$, were derived for 3 different experimental arrangements; each leading to a different characteristic PDE concentration profile. The expressions for signal range are related to the critical density measurements via the percolation relation, $\pi R^2 N^* = 4{\cdot}5$, relating signal range to critical cell density (Robertson & Cohen, 1974).

*PDE concentration profiles*

The PDE is continuously secreted by the population of amoebae on the agar surface (Gerisch *et al.* 1972). It diffuses into the agar which can be assumed to be of infinite volume because of the low PDE diffusion constant, $D_p$, less than $10^{-8}$ cm$^2$/s, as the agar blocks are 0·5 cm deep. The PDE concentration profile is then given by the solution of a one-dimensional equation with delta function source terms in $z$, the normal coordinate to the agar surface. The PDE concentration profiles are listed below for each of the 3 different experimental situations.

(i) For the $N^*$ vs. $N$ experiments there is simply a single population of amoebae secreting PDE. Their secretion from time zero to $t_R = 620'$, the time at which the field breaks up due to relaying, determines $N^*$. They secrete PDE at a constant rate, $G(N)$, and the concentration is

$$C_p(z) = \frac{G(N)zN}{D_p}\left(\sqrt{\left(\frac{4D_p t_R}{\pi z^2}\right)}\exp\left(-\frac{z^2}{4D_p t_R}\right) + \operatorname{erf}\left(\frac{z}{\sqrt{(4D_p t_R)}}\right) - 1\right). \quad (1)$$

Typical PDE concentration profiles are shown for various times after harvesting (Fig. 11).

(ii) For the $N^*$ vs. $t_D$ experiments there are 2 populations secreting PDE, a population of *D. discoideum* amoebae whose secretion begins at time zero and a population of D1 amoebae with secretion beginning at the delay time, $t_D$. The PDE secretion of both populations up to $t_R = 620'$ determines the value of $N^*$. As will be discussed later, the PDE secretion rate is a function of $N$ so that the *D. discoideum* amoebae secrete at a rate of $G(N^*)$ from time zero to $t_D$ while both populations secrete at $G(N)$ after $t_D$. The PDE concentration for this arrangement is

$$C_p(z) = \frac{G(N^*)\,zN^*(t_p)}{D_p}\left(\frac{e^{-A^2z^2}}{zA\sqrt{\pi}} - \frac{e^{-B^2z^2}}{zB\sqrt{\pi}} + \operatorname{erf}(zA) + \operatorname{erf}(zB)\right) + \frac{G(N)zN}{D_p}\left(\frac{e^{-B^2z^2}}{zB\sqrt{\pi}} + \operatorname{erf}(zB) - 1\right), \quad (2)$$

where $A = (4D_p t_R)^{-\frac{1}{2}}$ and $B = (4D_p(t_R - t_D))^{-\frac{1}{2}}$.

(iii) For the PDE addition experiments there are also 2 sources of PDE: the beef heart PDE applied to the agar surface over a brief period at time zero and the continually secreting amoebae. The concentration is given by

$$C_{\mathrm{p}}(z) = \frac{G(N)zN}{D_{\mathrm{p}}}\left(\sqrt{\left(\frac{4D_{\mathrm{p}}t_{\mathrm{R}}}{z^2\pi}\right)}\,\mathrm{e}^{-z^2/4D_{\mathrm{p}}t_{\mathrm{R}}} + \mathrm{erf}\left(\frac{z}{\sqrt{(4D_{\mathrm{p}}t_{\mathrm{R}})}}\right) - 1\right) + \frac{\eta_{\mathrm{p}}}{\sqrt{(\pi D_{\mathrm{p}}')}}\cdot\frac{\mathrm{e}^{-z^2/4D_{\mathrm{p}}'t_{\mathrm{R}}}}{\sqrt{t_{\mathrm{R}}}}, \quad (3)$$

where $\eta_{\mathrm{p}}$ is the real density of PDE applied at time zero and $D_{\mathrm{p}}'$ is the diffusion constant for beef heart PDE in 2 % agar.

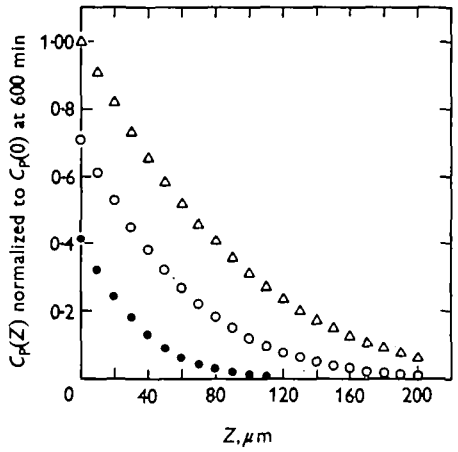


Fig. 11. Calculated PDE concentration profiles, $C_{\mathrm{p}}(Z)$, for a single population of secreting amoebae. —●—●—, 100′ after harvesting; —○—○, 300′ after harvesting; and —△—△—, 600′ after harvesting. $D_{\mathrm{p}} = 2{\cdot}25 \times 10^{-3}$ cm²/s. $Z$ = distance beneath agar surface.

*cAMP diffusion equation*

During the course of a signal, cAMP diffuses hemispherically from a single cell. The cAMP secretion area is taken to be small (Robertson & Cohen, 1974) so that the concentration profiles are given by a point source, hemispherical diffusion equation with an appropriate PDE sink term. The diffusion equation for cAMP concentration is then

$$D\nabla^2 C - \frac{\partial C}{\partial t} + 2\eta\delta(\mathbf{r})\,\delta(t) - (kC_{\mathrm{p}})\,C = 0, \quad (4)$$

where $D$ = cAMP diffusion constant in 2 % agar and $k$ = the product of the PDE–cAMP dissociation constant per site and the number of sites per molecule divided by the Michaelis–Menten constant for PDE in the system. The factor of 2 appears in the delta function source term in Eq. (4) to take account of the hemispherical diffusion of cAMP. Since $C_{\mathrm{p}}$ varies very slowly when compared with $C$, its time dependence is taken only parametrically. Eq. (4) cannot be solved analytically with any of the 3 PDE

concentration profiles of the previous section. However, Eq. (4) can be solved analytically with $1/\tau_0 = kC_p$ = constant. In this case the cAMP concentration is given by

$$C_0 = \frac{2\eta}{(4\pi Dt)^{\frac{3}{2}}} e^{-r^2/4Dt} e^{-t/\tau_0}. \tag{5}$$

Rough estimates of $D_p$ have been made from observed chemotactic ranges for artificial cAMP sources (Robertson & Drage, 1975). These give

$$2 \times 10^{-9}\,\text{cm}^2/\text{s} < D_p < 1{\cdot}4 \times 10^{-8}\,\text{cm}^2/\text{s}.$$

For $D_p$ in this range, the PDE concentrations near the surface vary slowly. In this case an iteration can be done in $\Delta C_p(z) = C_p(0) - C_p(z)$ which should be small enough near the surface to ensure accuracy.

*First-order corrections to $C_0$*

The Green's function of Eq. (4) with $kC_p = 1/\tau_0$ = constant is

$$G_0(r, t; r', t') = \frac{1}{(4\pi D)^{\frac{3}{2}}} \cdot \frac{\exp\left(-(r-r')^2/4D(t-t') - (t-t')/\tau_0\right)}{(t-t')^{\frac{3}{2}}}. \tag{6}$$

The Green's functions of Eq. (4) with the actual PDE concentration profiles were formulated via the Parametrix method (Friedman, 1964). They are of the form

$$G(r, t; r', t') = G_0(r, t; r', t') + G_1(r, t; r', t') + (\text{higher order terms}), \tag{7}$$

where

$$G_1(r, t; r', t') = k \iint d\mathbf{r}'' dt'' G_0(r, t; r'', t'') \Delta C_p(z'') G_0(r'', t''; r', t'). \tag{8}$$

For $\Delta C_p(z)$ small with respect to $C_p(0)$, the higher order terms can be neglected, yielding approximate expressions for $C(r, t)$ of the form

$$C(r, t) = C_0(r, t) + C_1(r, t), \tag{9}$$

where

$$C_1(r, t) = \iint d\mathbf{r}'\, dt' 2\eta\, \delta(\mathbf{r}')\, \delta(t')\, G_1(r, t; r', t'). \tag{10}$$

The cAMP concentration is given accurately by Eq. (9) if $\Delta C_p(z)$ is sufficiently small for $z < R$. A convenient measure of this is that $(C_1/C_0) \ll 1$.

Using Eqs. (8), (9), and (10) the cAMP concentration profiles can be calculated for each of the 3 PDE concentration profiles listed in Eqs. (1), (2), and (3). In all 3 cases the $C(r, t)$ has the form

$$C(r, t) = \eta F(t)\, e^{-r^2/4Dt}\, e^{-t/\tau_0}, \tag{11}$$

where $\tau_0$ is the relaxation time at the agar surface and the expressions for $F(t)$ are:

$$F(t) = -\left(\frac{kG(N)N}{(4\pi)^2 D^2 D_p A^2 t} + \frac{kG(N)N}{(4\pi)^2 D D_p}\right) \arctan\left(A\sqrt{(tD)}\right) + \frac{kG(N)N}{32\pi D D_p} + \frac{2}{(4\pi Dt)^{\frac{3}{2}}} - \frac{kG(N)N}{(4\pi)^2 D D_p A \sqrt{(tD)}} + \frac{1/\tau_0}{(4\pi D)^{\frac{3}{2}} t^{\frac{1}{2}}} \tag{12a}$$

for the $N^*$ vs. $N$ experiments with $C_p(z)$ given by Eq. (1),

$$F(t) = -\left(\frac{kG(N^*)N^*}{(4\pi)^2 D^2 D_p A^2 t} + \frac{kG(N^*)N^*}{(4\pi)^2 DD_p}\right)\arctan(A\sqrt{(tD)}) + \left(\frac{kG(N^*)N^*}{(4\pi)^2 D^2 D_p B^2 t} - \frac{kG(N)N}{(4\pi)^2 DD_p}\right)\arctan(B\sqrt{(tD)}) + \left(\frac{kG(N^*)N^*}{(4\pi)^2 DD_p} - \frac{kG(N)N}{(4\pi)^2 D^2 D_p B^2 t}\right)\arctan(B\sqrt{(tD)}) + \frac{k(G(N^*)N^* - G(N)N)}{(4\pi)^2 DD_p B\sqrt{(tD)}} - \frac{kG(N^*)N^*}{(4\pi)^2 DD_p A\sqrt{(tD)}} + \frac{kG(N)N}{32\pi DD_p} + \frac{2}{(4\pi D(t))^{\frac{3}{2}}} + \frac{1/\tau_0}{(4\pi D)^{\frac{3}{2}} t^{\frac{1}{2}}} \qquad (12b)$$

for the $N^*$ vs. $t_D$ experiments with $C_p(z)$ given by Eq. (2), and

$$F(t) = -\left(\frac{kG(N)N}{(4\pi)^2 D^2 D_p A^2 t} + \frac{kG(N)N}{(4\pi)^2 DD_p}\right)\arctan(A\sqrt{(tD)}) + \frac{kG(N)N}{32\pi DD_p} + \frac{2}{(4\pi Dt)^{\frac{3}{2}}} - \frac{kG(N)N}{(4\pi)^2 DD_p A\sqrt{(tD)}} + \frac{1/\tau_0}{(4\pi D)^{\frac{3}{2}} t^{\frac{1}{2}}} - \frac{k'\eta_p}{4\pi^2 D^2 t}\arctan(A\sqrt{(tD)}) \qquad (12c)$$

for the PDE addition experiments with $C_p(z)$ given by Eq. (3). Here $k$ corresponds to the slime mould PDE and $k'$ to the beef heart PDE.

The time, $t_m$, of the maximum cAMP concentration at the relay range is determined by setting the temporal derivative of Eq. (11) equal to zero with $r = R$. Then the relations between signal range and PDE secretion are

$$\left.\frac{\partial C(R,t)}{\partial t}\right|_{t=t_m} = 0 \qquad (13)$$

and

$$\frac{C^*}{\eta} = F(t_m)\exp\left(-\frac{R^2}{4Dt_m}\right)\exp\left(-\frac{t_m}{\tau_0}\right), \qquad (14)$$

where $C_{max}$ is set equal to $C^*$ at the signal range $R$.

## REFERENCES


ASHWORTH, J. M. & WATTS, D. J. (1970). Growth of myxamoebae of the cellular slime mould *Dictyostelium discoideum* in axenic culture. *Biochem. J.* **119**, 171–174.

BONNER, J. T. (1947). Evidence for the formation of cell aggregates by chemotaxis in the development of the slime mold. *J. exp. Zool.* **106**, 1–26.

BONNER, J. T. (1963). Epigenetic development in the cellular slime moulds. *Symp. Soc. exp. Biol.* **17**, 341–358.

BONNER, J. T. (1967). *The Cellular Slime Moulds*, 2nd edn. Princeton: Princeton University Press.

BONNER, J. T. & DODD, M. R. (1962). Aggregation territories in the cellular slime moulds. *Biol. Bull. mar. biol. Lab., Woods Hole* **122**, 13–24.

CHANG, YING-YING (1968). Cyclic 3′,5′-adenosine monophosphate phosphodiesterase produced by the slime mold *Dictyostelium discoideum*. *Science, N.Y.* **160**, 57–59.

COHEN, M. H. & ROBERTSON, A. (1971*a*). Wave propagation in the early stages of aggregation of cellular slime molds. *J. theor. Biol.* **31**, 101–118.

COHEN, M. H. & ROBERTSON, A. (1971*b*). Chemotaxis and the early stages of aggregation of cellular slime molds. *J. theor. Biol.* **31**, 119–130.

COHEN, M. H. & ROBERTSON, A. (1972). Differentiation for aggregation in the cellular slime molds. In *Cell Differentiation* (ed. R. Harris, P. Allin & D. Viza), pp. 35–45. Copenhagen: Munksgaard.

COHEN, M. H. & ROBERTSON, A. (1975). Cellular organization and communication in *Dictyostelium discoideum* and other cellular slime molds. In *NATO Advanced Study Institutes Series E*, vol. 9 (ed. E. R. Caianiello), pp. 217–240. Leyden: Noordhoff.

FRIEDMAN, A. (1964). *Partial Differential Equations of Parabolic Type*, chapter 1. London: Prentice-Hall.

GERISCH, G. (1968). Cell aggregation and differentiation in *Dictyostelium*. *Curr. Top. dev. Biol.* **3**, 157–197.

GERISCH, G., MALCHOW, D., RIEDEL, V., MULLER, E. & EVERY, M. (1972). Cyclic AMP phosphodiesterase and its inhibitor in slime mould development. *Nature, New Biol.* **235** (55), 90–92.

GINGLE, A. & ROBERTSON, A. (1975). The development of the relaying competence in *Dictyostelium discoideum*. *J. Cell Sci.* **20**, 21–27.

HASHIMOTO, Y., COHEN, M. H. & ROBERTSON, A. (1975). Cell density dependence of the aggregation characteristics of the cellular slime mould *Dictyostelium discoideum*. *J. Cell Sci.* **19**, 215–229.

HENDERSON, E. (1975). The cyclic-AMP receptor of *Dictyostelium discoideum*. *J. biol. Chem.* (in Press).

KONIJN, T. M., BARKLEY, D. S., CHANG, Y.-Y. & BONNER, J. T. (1968). Cyclic AMP: a naturally occurring acrasin in the cellular slime molds. *Am. Nat.* **102**, 225–233.

KONIJN, T. M. & RAPER, K. B. (1961). Cell aggregation in *Dictyostelium discoideum*. *Devl Biol.* **3**, 725–756.

MALKINSON, A. M. & ASHWORTH, J. M. (1973). Adenosine 3′:5′-cyclic monophosphate concentrations and phosphodiesterase activities during axenic growth and differentiation of cells of the cellular slime mould *Dictyostelium discoideum*. *Biochem. J.* **134**, 311–319.

RAPER, K. B. (1940). Pseudoplasmodia formation and organization in *Dictyostelium discoideum*. *J. Elisha Mitchell scient. Soc.* **56**, 241–282.

ROBERTSON, A. & COHEN, M. H. (1974). Quantitative analysis of the development of the cellular slime molds. II. *Lectures on mathematics in the Life Sci.* **6**, 44–62.

ROBERTSON, A. & DRAGE, D. (1975). Stimulation of late interphase *D. discoideum* amoebae with an external cyclic AMP signal. *Biophys. J.* **15** (8) (in Press).

ROBERTSON, A., DRAGE, D. & COHEN, M. H. (1972). Control of aggregation in *Dictyostelium discoideum* by an externally applied periodic pulse of cyclic AMP. *Science, N. Y.* **175**, 333–335.

SHAFFER, B. M. (1962). The Acrasina, Part I. *Adv. Morph.* **2**, 109–182.

SHANTE, V. K. & KIRKPATRICK, S. (1971). An introduction to percolation theory. *Adv. Phys.* **20**, 325–357.

SUSSMAN, M. & ENNIS, H. L. (1959). The role of the initiator cell in slime mold aggregation. *Biol. Bull. mar. biol. Lab., Woods Hole* **116**, 304–317.

SUSSMAN, M. & NOEL, E. (1952). An analysis of the aggregation stage in the development of the slime molds, Dictyosteliaceae. I. The population distribution of the capacity to initiate aggregation. *Biol. Bull. mar. biol. Lab., Woods Hole* **103**, 259–268.

SUSSMAN, M. & SUSSMAN, R. R. (1961). Aggregative performance. *Expl Cell Res.* **8**, 91–106.

(*Received* 13 *June* 1975)